Journal of Hazardous Materials 180 (2010) 173–180

Contents lists available at ScienceDirect

Journal of Hazardous Materials

journal homepage: www.elsevier.com/locate/jhazmat

Recycling of fly ash for preparing porous mullite membrane supports with titania addition

Yingchao Dong[a,*], Stuart Hampshire[a], Jian-er Zhou[b], Bin Lin[c], Zhanlin Ji[a], Xiaozhen Zhang[c], Guangyao Meng[c]

[a] Materials and Surface Science Institute (MSSI), University of Limerick, Castletroy National Technological Park, Limerick, Ireland
[b] Key Lab of Jiangxi Universities for Inorganic Membranes, National Engineering Research Center for Domestic and Building Ceramics, Jingdezhen Ceramic University (JCU), Jingdezhen, Jiangxi 333001, PR China
[c] USTC Lab for Solid State Chemistry and Inorganic Membranes, Department of Materials Science and Engineering, University of Science and Technology of China (USTC), Hefei, 230026, PR China

ARTICLE INFO

Article history:
Received 7 January 2010
Received in revised form 1 March 2010
Accepted 3 April 2010
Available online 10 April 2010

Keywords:
Fly ash
Waste recycling
Ceramic membrane supports
Sintering
Titania

ABSTRACT

In order to effectively utilize industrial waste fly ash, porous mullite ceramic membrane supports were prepared from fly ash and calcined bauxite with chemically pure titania as sintering additive. The effects of TiO_2 on the sintering behaviors and main properties of porous mullite were studied in detail. Due to the addition of titania, the sintering of the flyash-based mullite was inhibited at low temperatures, but effectively improved at high temperatures, the latter is suitable for preparing porous mullite membrane supports by incomplete sintering. Titania entered into liquid glassy phase with low high-temperature viscosity during sintering, resulting in the improvement of sintering activity, as well as the lowering of secondary mullitization temperature (where 2.0% titania). Between 1300 and 1500 °C, with increasing titania content, the samples exhibit increased trends in both linear shrinkage percent and bulk density, but a slightly decreased trend in open porosity, at all sintering temperatures. At 1300–1500 °C, the samples sintered at 1450 °C for 2 h exhibit the lowest shrinkage and bulk density, as well as the highest open porosities in the investigated titania content range of 0–6.0 wt.%. Also, with increasing titania content, the pore size decreases slightly but the three-point flexural strength increases gradually at 1450 °C.

1. Introduction

Waste fly ash is a residue found in waste after incineration of raw coal in thermal power plants. This industrial waste is regarded as hazardous material all over the world, which presents serious problems related to land disposal and environmental pollution. Therefore, the effective recycling of waste fly ash not only decreases environmental pollution, but also produces high value-added products. In recent years, there have been a great deal of research efforts made on recycling of this industrial waste for producing glass-ceramics with controllable crystalline phases [1–5], cordierite ceramics [6–8], and porous cordierite membrane where both layered porous micro-structure and multi-oxide crystalline phase could be effectively controlled at the one-step reaction sintering process [9]. However, there are few reports on preparation of porous mullite ceramics using waste fly ash.

Currently, commercialized porous ceramic membranes cannot fulfill strong environmental requirements such as massive liquid waste pre-treatment, strong alkaline media separation and thermal shock separation applications, due to their several drawbacks including high cost, rare membrane materials and narrow application range. In recent years, porous mineral-based ceramic membranes have attracted much attention in the scientific community for their outstanding merits such as low cost, species diversity and good additional properties [10,11]. Recently, some new ceramic membrane types and applications have been developed [12–19]. These ceramic membranes are expected to be used in some separation applications due to their low cost, especially where the requirements of membrane performances are not harsh.

Recycling of waste fly ash for use in preparation of porous ceramic membrane is also helpful in conservation of the environment. Generally, the components of waste fly ash are complex and unfixed, of which the physical and chemical properties depend on the type of raw coal, as well as combustion conditions. Fly ash, in which silica (SiO_2) and alumina (Al_2O_3) are main components associated with minor amount of other metallic oxides, is very suitable for production of mullite ceramics [20]. In our previous work related to synthesis of dense mullite from fly ash and bauxite mineral [21], it was found that a unique self-expansion occurred before full densification due to

* Corresponding author. Tel.: +353 61202640; fax: +353 61338172.
E-mail addresses: yingchao.dong@ul.ie, dongyc9@mail.ustc.edu.cn (Y. Dong).

0304-3894/$ – see front matter © 2010 Elsevier B.V. All rights reserved.
doi:10.1016/j.jhazmat.2010.04.010

the high-temperature secondary mullitization reaction. It is further justified that this sintering expansion behavior had a positive effect on the porous structure of mullite, especially improvement of porosity and pore size. Then we prepared porous mullite membrane supports without any pore-forming additives, only via the contribution of this sintering expansion to micro-structure [22]. Nevertheless, there are still unrevealed research topics on the development of porous flyash-based mullite membrane supports by improving their performances, especially lowering sintering temperature. As discussed [21,22], two factors can influence the sintering of the mixture of bauxite and waste fly ash: one is secondary mullitization; the other is the amount of liquid glassy phase. Secondary mullitization is accompanied with a volume expansion, resulting in increased open porosity at elevated temperatures. On the contrary, liquid glassy phase could promote sintering, causing a decreased porosity. Therefore, it is very essential to adopt suitable sintering additive in order to lower sintering temperature of mullite membrane support by a newly formed liquid phase, without degradation of other properties significantly.

Low-temperature sintering via sintering aids is a quite important method to reduce fabrication cost of porous mullite. Most of the past research has been made to lower sintering temperature in order to obtain dense mullite by the liquid-phase process with different sintering aids such as MgO, SrO, TiO_2, Fe_2O_3, CeO_2, and YSZ [23–26].

In the current work, porous mullite membrane support was fabricated by recycling of waste fly ash and bauxite with titania as sintering additive. The effects of sintering aid TiO_2 on the main properties of porous mullite were studied in detail, mainly including sintering behavior, phase compositions, micro-structure, pore-structure and mechanical properties.

2. Experimental procedure

2.1. Starting materials

Industrial waste fly ash and calcined high-Al bauxite powders were used as starting materials in order to prepare porous mullite membrane supports. Chemically pure titania was used as sintering additive. Fly ash powder was obtained from Hefei No. 2 thermal power plant (Hefei, Anhui Province, P.R. China). Calcined high-Al bauxite powder was purchased from Yangquan city (Shanxi Province, P.R. China). The mixture of fly ash and calcined bauxite, based on the composition of 3:2 mullite ($W_{\text{fly ash}}$:W_{bauxite} = 56.73:100), was wet-mixed for 12 h with water as medium using polyurethane-coated steel balls in a polyethylene pot. The 3:2 mullite, i.e., $Al_2[Al_{2.5}Si_{1.5}]O_{9.75}$, is considered to be the most stable phase among other types (2:1 mullite and 3:1 mullite). It also has a highly stable open structure ($T_{\text{Melt}} = 1828 \pm 10\,^{\circ}C$) and it can accommodate a variety of transition metal ions into its structure as a solid solution [27].

After drying, the mixture powder was uniformly mixed with 20 wt.% titania aqueous suspensions in a ceramic mortar for 1 h, respectively, based on four mass ratios (0 wt.%, 2 wt.%, 4 wt.% and 6 wt.%). After sufficient drying at 120 °C, the bulk mixtures were slightly crushed into powders by hand in a mortar.

2.2. Pressing and sintering

The mixture powders with different titania contents were slightly crushed to break the agglomerates, mixed with organic binder PVA-1750 (5.00 wt.% solution) and then uniaxially pressed at a pressure of 160 MPa. Both rectangular bars (50 mm × 6 mm × 3–4 mm) and cylindrical pellets (25 mm in diameter and 2–3 mm in height) were made in two different stainless steel moulds. After drying, the samples were fired at various temperatures between 1300 and 1500 °C at an interval of 50 °C for 2 h. Firing was carried out in a preprogrammed automatic control electric furnace and the heating rate was 1 °C min^{-1} up to 450 °C, and 2 °C min^{-1} up to final temperatures. A holding time of 1 h was carried out at 450 °C in order to remove added organic additives.

2.3. Characterization techniques

The particle size distribution of the mixture of fly ash and bauxite was determined using a laser particle size analyzer (Rise-2006, Jinan Rise Science & Technology Co. Ltd., P.R. China) using PEG-10000 (polyethylene glycol; molecular weight: 10,000 g mol^{-1}) as organic dispersing agent.

Sintering shrinkage behaviors of the green rectangular bars of the mixtures of bauxite and fly ash with different titania contents were respectively measured between room temperature (26 °C) and 1550 °C in a horizontal dilatometer (DIL 402C, Netzsch, Germany). A constant heating rate of 5 °C min^{-1} was used. Length change was recorded with a dense α-alumina as reference sample. Both raw materials and sintered samples were directly characterized using XRD (D8 ADVANCE, Bruker Corporation, Germany; Cu Kα radiation). The shrinkage percents in diameter direction of the sintered cylindrical pellets were measured using a vernier caliper. In addition, both bulk density and open porosity were measured in distilled water medium using a conventional method according to the Archimedes' principle.

Pore size distributions were examined in a lab-made equipment according to the bubble-point method, which is on the basis of gas–liquid replacement mechanism. Micro-structures of the sintered bodies were observed using FE-SEM (Field Emission Scanning Electronic Microscope; JSM-6700F, JEOL, Japan) after sputtering gold coating on cross-sectional surfaces. Room temperature flexural strength was determined by the three-point bending method in a universal materials testing machine (3369, Instron Corporation, USA). A span length of 30 mm and a crosshead speed of 0.5 mm min^{-1} were used. All the tested bars were polished and beveled in advance by 360-mesh and then 800-mesh metallographic sandpapers in order to eliminate surface stress. Fracture strength was calculated according to the following expression (ISO9693 1999).

$$\sigma = \frac{3P \times l}{2b \times h^2}$$

where σ is fracture strength (Pa), P is fracture load (N), l is span length (m), b is width of sample (m), h is height of sample (m).

3. Results and discussion

3.1. Characterization of starting materials

The chemical composition and crystalline phase analysis of fly ash were described in our previous work [21]. The detected major crystalline phases are mullite ($3Al_2O_3{\cdot}2SiO_2$, orthorhombic system, PDF# 79-1455) and α-quartz (SiO_2, hexagonal system, PDF# 85-0797). Amorphous silicate glassy phase was also detected, which is derived from uncrystallized silica-rich substance due to the rapid cooling process during combustion. Regarding chemical composition, the majority of fly ash consists of SiO_2 (57.40 wt.%) and Al_2O_3 (31.35 wt.%). In addition to transition metal oxides (2.86 wt.% Fe_2O_3 and 1.37 wt.% TiO_2), there are also small amounts of co-existing alkali and alkaline-earth metal oxides such as Na_2O, K_2O, MgO, CaO, etc.

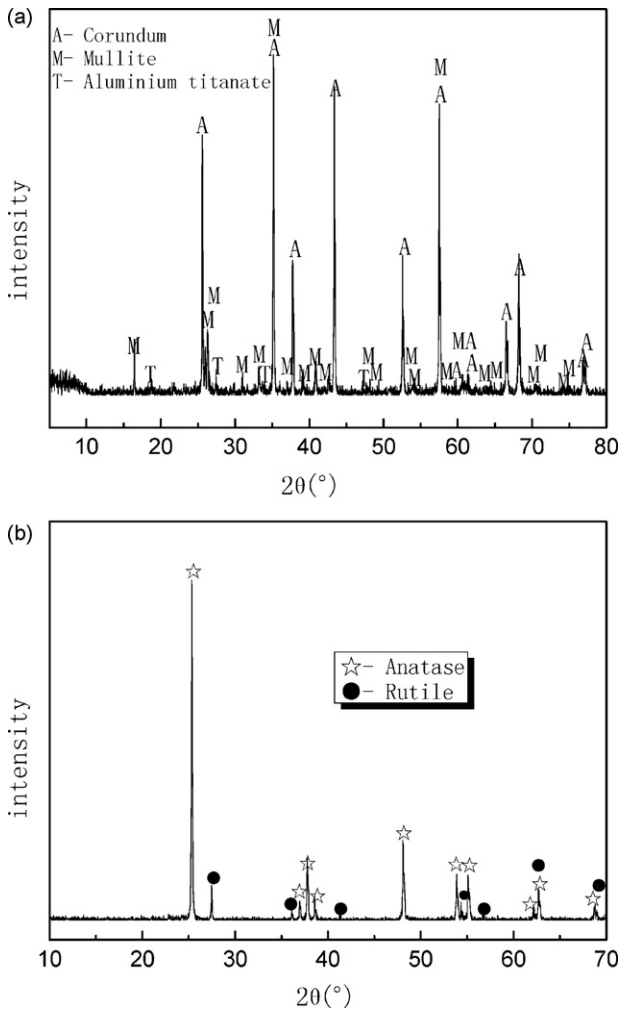

Fig. 1. XRD patterns of the starting materials: (a) calcined bauxite powder, and (b) chemically pure titania powder.

Fig. 1 illustrates the XRD patterns of the as-received calcined bauxite and chemically pure titania powders. The major crystalline phase is α-alumina (Al_2O_3, cubic system, PDF#79-1558) in the calcined bauxite (Fig. 1a). In contrast, mullite ($3Al_2O_3{\cdot}2SiO_2$, orthorhombic system, PDF# 79-1455) exists as a minor crystalline phase. And very minor amount of aluminum titanate ($Al_2O_3{\cdot}TiO_2$, orthorhombic system, PDF# 81-0030) was detected as a second minor phase, according to its very weak diffraction peaks in the XRD pattern. Aluminum titanate was formed between rutile and corundum during the high-temperature calcination of raw high-Al bauxite mineral [28]. From the XRD pattern in Fig. 1b, it is noted that for chemically pure titania there are two crystalline types of titania, i.e., anatase (as major phase) and rutile (as minor phase). The chemical composition of the as-received bauxite was characterized by XRF, and the results are listed in Table 1. Bauxite is of high-Al content, mainly composed of 85.36 wt.% alumina. There is a certain amount of silica (7.89 wt.%) and titania (3.85 wt.%). In association with Fig. 1a, it is known that titania exists in the form of aluminum titanate. The content of ferric oxide is very little (1.52 wt.%). A very small amount of other oxides such as MgO, K_2O, CaO, Cr_2O_3, MnO, NiO_2, and ZrO_2, were also detected.

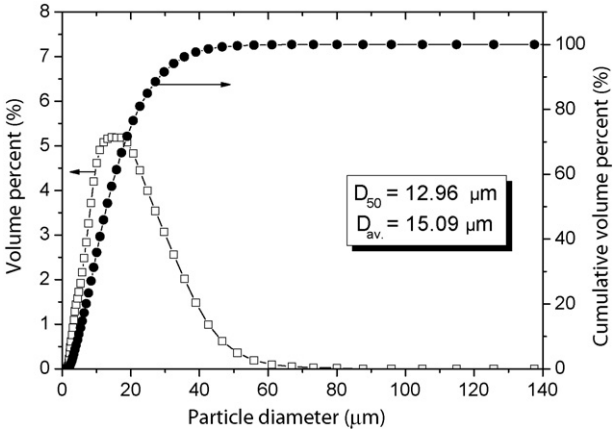

Fig. 2. Particle size distribution of the as-used calcined bauxite powder.

Fig. 2 shows the particle size distribution of the ball-milled mixture of fly ash and calcined bauxite. As can be seen, the average particle diameter is 15.09 μm, with majority of particles falling between 9.00 and 24.00 μm in diameter.

3.2. *Effects of TiO_2 on sintering shrinkage behaviors*

Fig. 3 displays the sintering shrinkage behaviors of the flyash–auxite mixture samples with various titania contents (0–6 wt.%). For the sample without titania addition, at high temperatures, the sintering process could be divided into three stages, which were described in detail in our previous work [22]. More especially, a unique sintering self-expansion stage was observed in the range of 1280–1510 °C. At this stage, the secondary mullitization reaction was caused by the dissolution of corundum into transient glassy liquid phase, followed by the precipitation of mullite crystals [29]. This mullitization reaction predominated the micro-structure change during high-temperature sintering of samples, in spite of gradual densification via liquid-phase sintering. The latter is a general phenomenon in many ceramic systems.

By contrast, the samples with titania addition exhibit similar sintering shrinkage behaviors with that without titania. But the difference in sintering shrinkage is still observed, just described as follows:

(a) The first sintering shrinkage stage. The sample without titania began to shrink at 875 °C and then ceased to shrink at 1280 °C. But the initial shrinkage temperatures are delayed to higher temperature for all the samples with titania addition. The initial shrinkage temperatures are respectively 934, 935 and 930 °C for the samples containing 2 wt.%, 4 wt.% and 6 wt.% titania. In particular, for the samples containing titania, the relative slight

Table 1
Quantitative X-ray fluorescence spectral analysis of the as-received calcined bauxite.

	Chemical composition (wt.%) of calcined bauxite										
Compound	Al_2O_3	SiO_2	MgO	K_2O	CaO	TiO_2	Cr_2O_3	MnO	Fe_2O_3	NiO	ZrO
	85.36	7.89	0.23	0.22	0.14	3.85	0.29	0.02	1.52	0.02	0.16
Element	Al	Si	Mg	K	Ca	Ti	Cr	Mn	Fe	Ni	Zr
	45.18	3.69	0.14	0.18	0.10	2.31	0.20	0.01	1.06	0.01	0.12

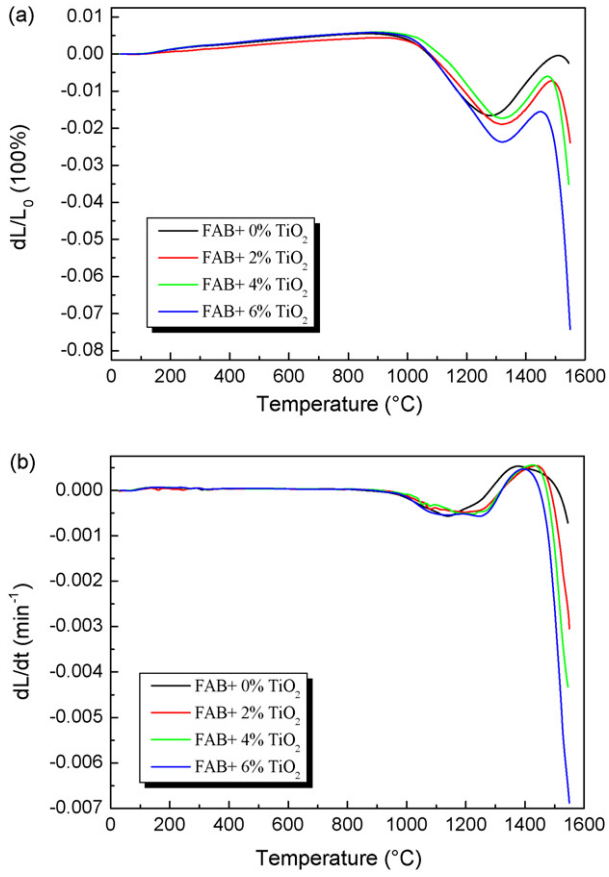

Fig. 3. Linear shrinkage percent dL/dL_0 (a) and differential linear shrinkage percent dL/dt (b) of the porous mullite samples with different TiO_2 contents.

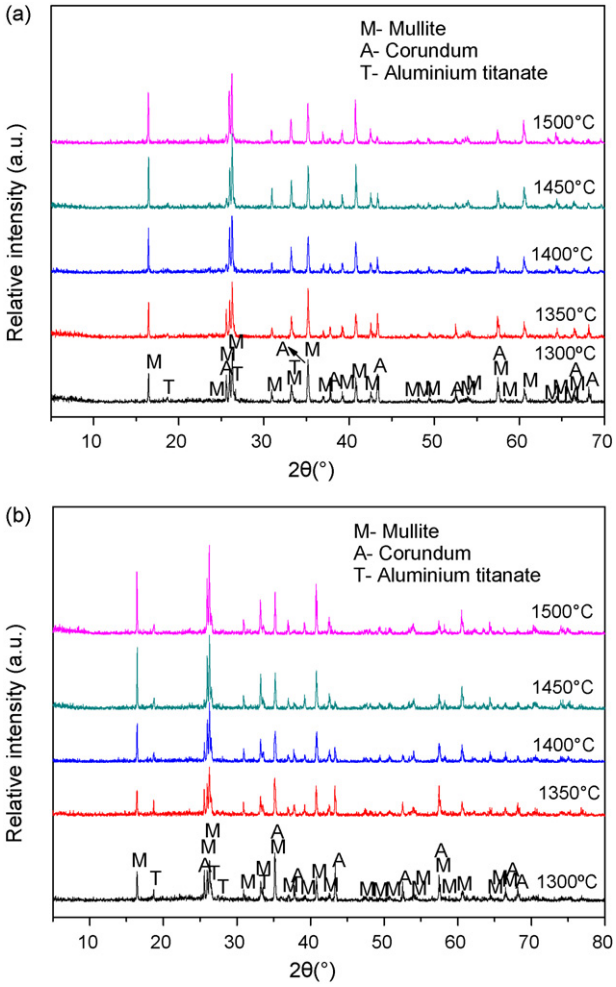

Fig. 4. XRD patterns of porous mullite samples after sintering at different temperatures for 2 h: (a) 2 wt.% TiO_2; (b) 6 wt.% TiO_2.

increases of dL/L_0 in this first shrinkage stage could be ascribed to the decreased sintering activity of samples due to the addition of titania. This is because chemically pure titania filling in the porous compacts was inert and un-reacted at this temperature range. It is concluded that the addition of titania slightly inhibited the sintering of fly ash and bauxite at low temperatures.

(b) The second sintering expansion stage. The sintering expansion stage of the sample without titania is in the temperature range of 1280–1510 °C. But the sintering expansion occurred at 1320–1487 °C, 1319–1473 °C, 1321–1450 °C for the samples with additions of 2 wt.%, 4 wt.% and 6 wt.% titania. Initial expansion temperatures are also delayed to higher temperature for all the samples containing titania because the added titania reacted with alumina substance to form aluminum titanate with low sintering activity, resulting in the decrease in sintering ability of the samples. But ending temperatures of sintering expansion stage, i.e., the initial temperatures of the third sintering re-shrinkage stage, decrease with increasing titania content. This can be ascribed to that the titania-rich glassy liquid phase, formed from titania and silica-based glassy phase in raw materials, promoted the sintering of the flyash/bauxite sample. As a consequence, the samples containing titania exhibit higher sintering shrinkage percents than the one without titania in this sintering stage, indicating that the addition of titania could promote the sintering to different degrees.

(c) The third sintering shrinkage stage. The sample without titania began to shrink at about 1510 °C at this third stage. By comparing the shrinkage curves of the samples with and without titania, it is noted that all the samples containing titania began to shrink at lower temperatures (1487 °C at 2 wt.%, 1473 °C at 4 wt.%,1450 °C at 6 wt.%,). More especially, the titania-contained samples show much higher shrinkage percents and quicker shrinkage rates, which is more obvious when increasing temperature. The lower initial shrinkage temperature, associated with higher shrinkage percents and quicker shrinkage rates, indicates again that the sintering activity at high-temperature region could be effectively improved by adding titania powder into the mixture of fly ash and bauxite. The values of shrinkage percent are 4.82×10^{-4}, 7.75×10^{-3}, 8.87×10^{-3} and 2.53×10^{-2} respectively, for the samples with 0 wt.%, 2 wt.%, 4 wt.% and 6 wt.% titania at 1500 °C.

3.3. Effects of TiO_2 on main properties of porous mullite

3.3.1. XRD patterns

Fig. 4 shows the XRD patterns of the porous mullite-based supports containing 2 wt.% and 6 wt.% TiO_2 after sintering at different temperatures (1300–1500 °C) for 2 h. For the mere flyash/bauxite mixture sintered at 1300–1450 °C, the peak intensity of corundum phase gradually decreases, and almost approaches to zero at 1450 °C because it dissolved into transient liquid glassy phase for further secondary mullitization reaction. Mullite is only crystalline phase present in the samples above 1450 °C [22].

From Fig. 4a, it can be seen that no aluminum titanate phase is observed above 1350 °C. With the addition of 2 wt.% titania, corundum phase appears at 1300 and 1350 °C, then disappears almost at 1400 °C. At 1400-1500 °C, the diffraction peaks of corun-

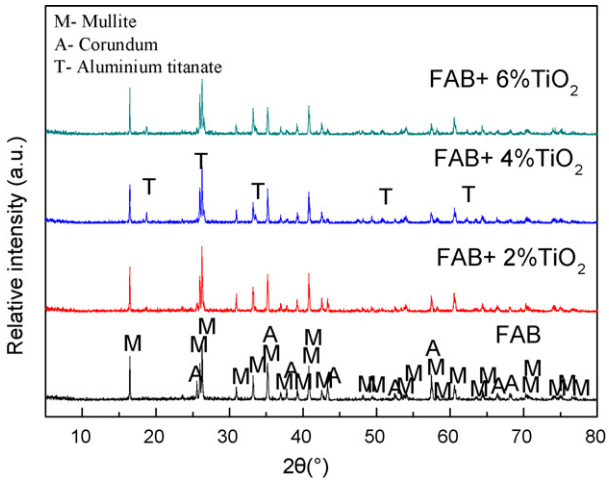

Fig. 5. XRD patterns of the flyash-based porous samples with various TiO_2 contents (0–6 wt.%) after sintering at 1450 °C for 2 h.

dum are very weak, indicating that the only crystalline phase is mullite. This indicates that the addition of titania could effectively promote the mullitization reaction between corundum and silica-rich glassy phase at lower sintering temperatures. TiO_2, as a nucleating agent, facilitated the nucleation of acicular mullite, and its subsequent growth for promoting crystallization of secondary mullite in the porous mullite sintered bodies. According to the SiO_2–Al_2O_3–TiO_2 ternary system phase diagram, titania entered into the liquid glassy phase at high temperatures when the total amount of titania (including existing titania in raw materials and added chemically pure titania) reached its solid-solution limit in mullite lattice [30–32]. Therefore, a low-viscosity titania-containing glassy liquid phase was formed, which accelerated the reaction diffusion between corundum and silica-rich glassy phase, as well as the precipitation of mullite crystals from transient liquid glassy phase. This results in a much lower completion temperature of mullitization reaction.

From Fig. 4b, it is seen that corundum phase appears at 1300–1400 °C, then disappears approximatively at 1450 °C, suggesting that the mullitization reaction completion temperature of the sample containing 6 wt.% titania is 1450 °C. At 1500 °C, no corundum diffraction peaks are observed. Also, aluminum titanate phase is observed at all sintering temperatures between 1300 and 1500 °C. This XRD results indicate that an excessive amount of added titania did not promote the mullitization reaction, but resulted in the production of aluminum titanate phase. Even though at high temperatures, aluminum titanate still exists maybe because some small amount of transition metal and alkaline-earth metal oxides (in the staring materials) entered into the lattices of aluminum titanate, and therefore inhibited its decomposition into titania and alumina. In this case, the excessive titania also entered into liquid glassy phase and resulting in the production of more amount of liquid glassy phase with lower high-temperature viscosity. As a consequence, the sintering of the sample with 6 wt.% titania was improved due to the addition of titania.

Fig. 5 shows the XRD patterns of the samples with various TiO_2 contents (0–6 wt.%) after sintering at 1450 °C for 2 h. For all the samples, mullite is major crystalline phase. Corundum phase appears for the sample without titania, but disappears almost for the sample with 2–6 wt.% titania. This suggests again that the addition of titania could effectively promote secondary mullitization reaction at 1450 °C. Mullite is a only crystalline phase in the sample with 2.0 wt.% titania. But for the samples with high titania content (4.0 wt.% and 6.0 wt.%), aluminum titanate was detected as a minor phase.

3.3.2. Shrinkage percent and bulk density

Fig. 6 presents the diameter shrinkage percent and bulk density of the flyash-based porous mullite compacts sintered at 1300–1500 °C for 2 h. For all the samples, both shrinkage percent and bulk density are increased with titania content at all the sintering temperatures, suggesting again that the addition of titania could cause the densification sintering of the porous mullite compacts to some degree. The increase of cation mobility by the formation of cation vacancy caused by the substitution of Al^{3+} by Ti^{4+}, as well as the formed low-viscosity titania-containing glassy liquid phase could improve the sintering activity of the flyash/bauxite based porous mullite, resulting in the same porosities at lower thermal-treating temperatures, compared with the sample without titania addition. This is similar with the positive effect of titania on sintering of sillimanite-based mullite [33].

Sintering expansion behavior is also observed for the samples containing 0.0–6.0 wt.% titania. The decreases in both shrinkage percent and bulk density are observed at 1300–1450 °C. From this result, it is also concluded that the unique volume expansion sintering of all the samples, is in the temperature range of 1300–1450 °C. This is slightly different from the above dilatometric results because of the difference in thermal-treating schedule. During dilatometric measurement the hysteresis effect of densification took place for the samples fired at a quick heating rate (5 °C min^{-1}) without holding time. On the other hand, both low heating rate (2 °C min^{-1}) and thermal retardation (2 h) at every final temperature could enhance the densification level for the samples sintered in elec-

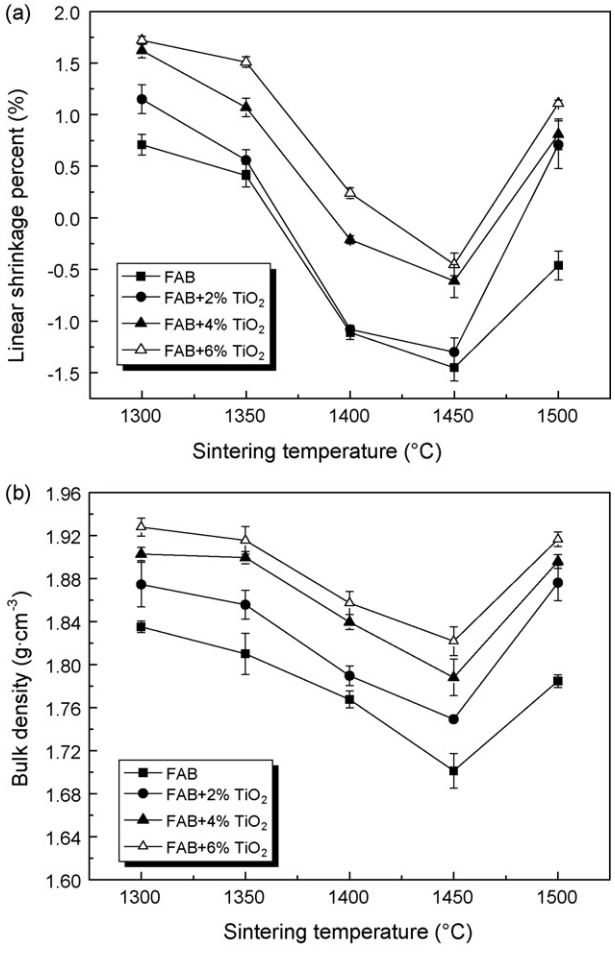

Fig. 6. Diametrical shrinkage percents (a) and bulk density (b) of the porous mineral-based mullite membrane supports with various TiO_2 contents after sintering at different temperatures between 1300 and 1500 °C for 2 h.

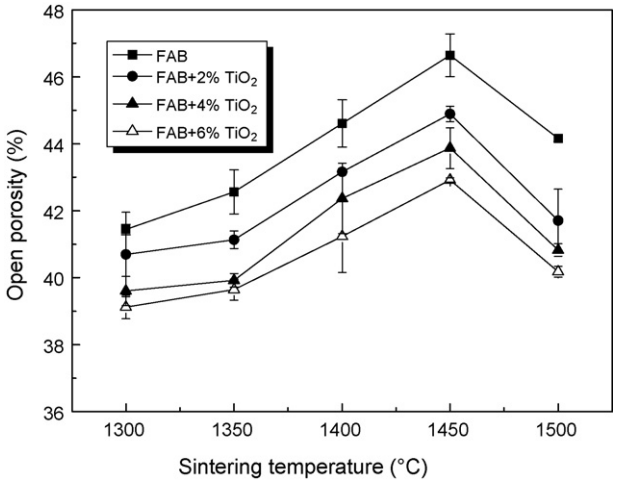

Fig. 7. Open porosity of the flyash-based mullite sintered bodies added with different TiO_2 as a function of sintering temperature.

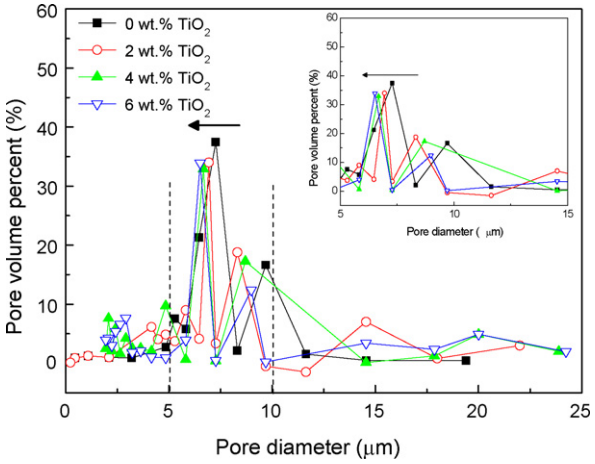

Fig. 8. Pore size distribution curves of flyash-based porous mullite supports with various TiO_2 contents after sintering at 1450 °C for 2 h.

tric furnace. With increasing sintering temperature further from 1450 to 1500 °C, the samples exhibit a characteristic of relatively quick densification at all titania levels, which is well verified by the quick increase in both radial shrinkage percent and bulk density. As can be seen, all the samples exhibit the lowest radial shrinkage percents (actually the highest expansion percents) and the lowest bulk density at 1450 °C for 2 h when sintered between 1300 and 1500 °C.

The as-prepared porous mullite membrane supports have a very low bulk density. Between 1300 and 1500 °C, average bulk density is in the range of 1.70–1.84 g cm^{-3}, 1.74–1.88 g cm^{-3}, 1.78–1.91 g cm^{-3}, 1.82–1.93 g cm^{-3} for the samples with 0 wt.%, 2 wt.%, 4 wt.% and 6 wt.% titania.

3.3.3. Open porosity

Fig. 7 shows the variation in open porosity in relation to the content of titania at different sintering temperatures (1300–1500 °C). The result of open porosity is in good agreement with that of sintering shrinkage percent and bulk density. For all the samples, the open porosity is slightly decreased with titania content when sintered at the same temperatures between 1300 and 1500 °C. A gradual increase in open porosity with temperature is observed for all the samples with the same titania doping levels sintered at 1300–1450 °C. The samples sintered at 1450 °C for 2 h exhibit the highest open porosities in the investigated titania content range of 0–6.0 wt.%. The open porosities are respectively 46.64 ± 0.64%, 44.89 ± 0.23%, 43.87 ± 0.61% and 42.92 ± 0.06% for the samples containing 0 wt.%, 2 wt.%, 4 wt.%, and 6 wt.% titania. The samples containing titania still show relatively high open porosity, which is very suitable for the application in filtration. But a decrease in open porosity is obtained at a higher sintering temperature (1500 °C) due to the occurrence of a sintering re-densification. Therefore, the porosity of the porous mullite supports could be effectively adjusted by choosing the above main parameters, including titania content and sintering temperature. The samples sintered at 1450 °C were selected due to relatively high open porosities and characterized by pore size and mechanical strength.

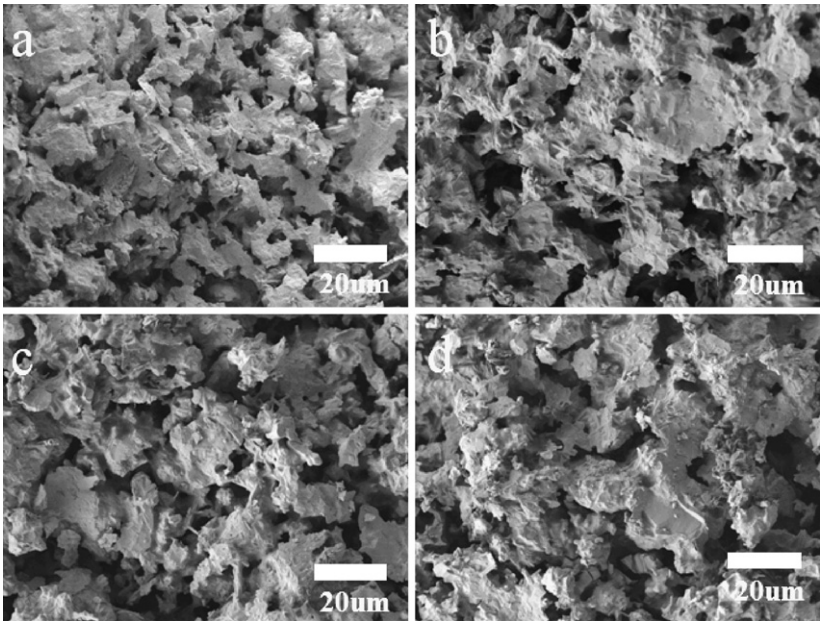

Fig. 9. Cross-sectional SEM microphotographs of the flyash-based porous mullite samples sintered at 1450 °C for 2 h with various TiO_2 contents: (a). 0 wt.% TiO_2; (b). 2 wt.% TiO_2; (c). 4 wt.% TiO_2; (d). 6 wt.% TiO_2.

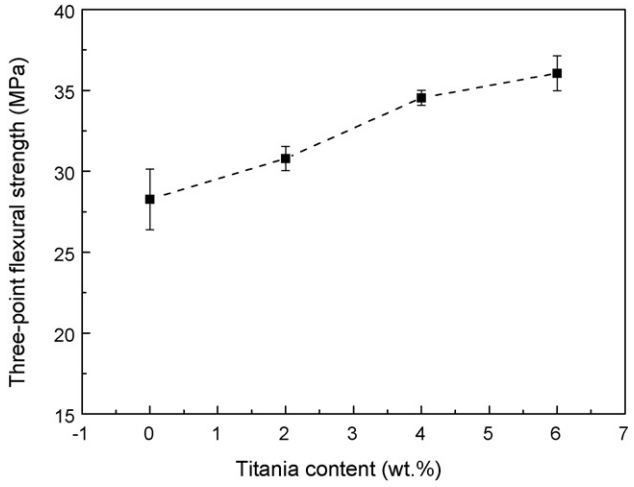

Fig. 10. The variation in three-point flexural strength with TiO_2 contents (0–6 wt.%) of the sintered flyash-based porous mullite supports.

3.3.4. Pore size distribution

Fig. 8 shows the pore size distributions of the mullite supports with different titania contents (0–6.0 wt.%) sintered at 1450 °C for 2 h. All the samples exhibit similar bimodal distributions of pore size. With increasing titania content from 0 to 6.0 wt.%, the average pore diameter decreases from 7.28 to 6.52 μm. This could be ascribed to the increased open pore shrinkage due to the generation of much more glassy liquid phase during sintering when increasing titania contents, though the thickness difference of the measured samples has a slight effect on pore size according to the Hagen–Posieuille equation during the bubble-point measurement based on a gas–liquid replacement mechanism [34].

Fig. 9 displays the SEM micro-structure photos of the flyash-based porous mullite samples with various titania contents (0–6 wt.%) sintered at 1450 °C for 2 h. A typical porous structure is observed for all the samples in spite of its titania content. With increasing titania content from 0 to 6 wt.%, a slight gradual densification took place because of the generation of more liquid glassy phase with lower high-temperature viscosity. The viscous flow sintering occurred as a result of a large amount of liquid phase [35]. This is also effectively verified by the formation of sintered particles with more smooth surfaces. According to the Al_2O_3–SiO_2 binary phase diagram, liquid phase can be formed at above eutectic temperature (1590 ± 10 °C) [36]. In our study, a mass of liquid glassy phase appeared at a relatively low-temperature mainly due to the increase of the amount of glassy phase by the dissolution of TiO_2. Also, the co-existing alkali and alkaline-earth metal oxides in raw materials (Table 1), acted as glass modifiers, not only lowered the viscosity of liquid glassy phase by forming weak Si–O bonds but also changed its wetting characteristic during sintering.

3.3.5. Mechanical strength

Fig. 10 shows the three-point flexural strengths of the selected porous mullite ceramics sintered at 1450 °C for 2 h. With increasing titania content, the slight improvement of flexural strength is ascribed to the enhanced densification of the porous mullite ceramic membrane supports. This supports the result of decreasing trend in porosity with increasing titania content. After sintering at 1450 °C for 2 h, the porous mullite exhibits three-point flexural strength values of 28.27 ± 1.87, 30.79 ± 0.74, 34.54 ± 0.46, 36.05 ± 1.08 MPa at room temperature for 0 wt.%, 2 wt.%, 4 wt.% and 6 wt.% titania additions.

4. Conclusions

In this work, porous mullite ceramic membrane supports were prepared from fly ash and calcined bauxite with titania as sintering additive. Due to the addition of titania, the sintering activity of the flyash-based mullite was inhibited at low temperatures, but effectively improved at high temperatures. Moreover, the sintering ability is increased with increasing titania content. This can be ascribed to that titania entered into liquid glassy phase with lower high-temperature viscosity during sintering, resulting in the improvement of sintering activity, as well as the lowering of secondary mullitization reaction temperature (especially for the sample with 2.0 wt.% titania). Between 1300 and 1500 °C, with increasing titania content, the samples exhibit increased trends in both linear shrinkage percent and bulk density, but a slightly decreased trend in open porosity, at all sintering temperatures. At 1300–1500 °C, the samples sintered at 1450 °C for 2 h exhibit the lowest shrinkage and bulk density, as well as the highest open porosities in the titania content range of 0–6.0 wt.%. When increasing titania content, the pore size decreases slightly but the three-point flexural strength increases at 1450 °C due to the aid-sintering function of titania.

Acknowledgement

The authors wish to thank the Irish Research Council for Science, Engineering and Technology (IRCSET) for the financial support (IRCSET EMPOWER post-doctoral grant).

References

[1] J.MA. Rincàn, M. Romero, A.R. Boccaccni, Microstructural characterisation of a glass and a glass-ceramic obtained from municipal incinerator fly ash, J. Mater. Sci. 34 (1999) 4413–4423.
[2] F. Peng, K.M. Liang, A.M. Hu, Nano-crystal glass–ceramics obtained from high alumina coal fly ash, Fuel 84 (2005) 341–346.
[3] Z. Károly, I. Mohai, M. Tóth, F. Wéber, J. Szépvölgyi, Production of glass-ceramics from fly ash using arc plasma, J. Eur. Ceram. Soc. 27 (2007) 1721–1725.
[4] J.M. Kim, H.S. Kim, Processing and properties of a glass-ceramic from coal fly ash from a thermal power plant through an economic process, J. Eur. Ceram. Soc. 24 (2004) 2825–2833.
[5] J.M. Kim, H.S. Kim, Glass-ceramic produced from a municipal waste incinerator fly ash with high Cl content, J. Eur. Ceram. Soc. 24 (2004) 2373–2382.
[6] Y. He, W.M. Cheng, H.S. Cai, Characterization of α-cordierite glass-ceramics from fly ash, J. Hazard. Mater. 120 (2005) 265–269.
[7] S. Kumar, K.K. Singh, P. Ramachandrarao, Synthesis of cordierite from fly ash and its refractory properties, J. Mater. Sci. 19 (2000) 1263–1265.
[8] H. Shao, K.M. Liang, F. Zhou, G.L. Wang, F. Peng, Characterization of cordierite-based glass-ceramics produced from fly ash, J. Non-Cryst. Solids 337 (2004) 157–160.
[9] Y.C. Dong, X.Q. Liu, Q.L. Ma, G.Y. Meng, Preparation of cordierite-based porous ceramic micro-filtration membranes using waste fly ash as the main raw materials, J. Membr. Sci. 285 (2006) 173–181.
[10] S. Masmoudi, R. Ben Amar, A. Larbot, H. El Feki, A. Ben Salah, L. Cot, Elaboration of inorganic microfiltration membranes with hydroxyapatite applied to the treatment of wastewater from sea product industry, J. Membr. Sci. 247 (2005) 1–9.
[11] S. Khemakhem, R. Ben Amar, A. Larbot, Synthesis and characterization of a new inorganic ultrafiltration membrane composed entirely of Tunisian natural illite clay, Desalination 206 (2007) 210–214.
[12] M.R. Weir, E. Rutinduka, C. Detellier, C.Y. Feng, Q. Wang, T. Matsuura, R. Le VanMao, Fabrication, characterization and preliminary testing of all-inorganic ultra-filtration membranes composed entirely of a naturally occurring sepiolite clay mineral, J. Membr. Sci. 182 (2001) 41–50.
[13] M.C. Almandoza, J. Marchese, P. Prádanos, L. Palacio, A. Hernández, Preparation and characterization of non-supported microfiltration membranes from aluminosilicates, J. Membr. Sci. 241 (2004) 95–103.
[14] J. Bentama, K. Ouazzani, Z. Lakhliai, M. Ayadi, Inorganic membranes made of sintered clay for the treatment of biologically modified water, Desalination 168 (2004) 295–299.
[15] J. Bentama, K. Ouazzania, P. Schmitzb, Mineral membranes made of sintered clay: application to crossflow microfiltration, Desalination 146 (2002) 57–61.
[16] A. Hinkova, I. Bohacenko, Z. Bubnik, M. Hrstkova, P. Jankovska, Mineral membrane filtration in refinement of starch hydrolysates, J. Food Eng. 61 (2004) 521–526.

[17] Y.F. Liu, X.Q. Liu, H. Wei, G.Y. Meng, Porous mullite ceramics from national clay produced by gel-casting, Ceram. Int. 27 (2001) 1–7.
[18] X.B. Zhang, Y.Z. Jiang, X.Q. Liu, G.Y. Meng, Sintering kinetics of ceramic from diatomite, J. Am. Ceram. Soc. 88 (2005) 1826–1830.
[19] S. Rakib, M. Sghyar, M. Rafiq, A. Larbot, L. Cot, New porous ceramics for tangential filtration, Sep. Purif. Technol. 25 (2001) 385–390.
[20] L.D. Hulett JR., A.J. Weinberger, K.J. Northcutt, M. Fergusone, Chemical species in fly ash from coal-burning power plants, Science 210 (1980) 1356–1358.
[21] Y.C. Dong, X.Y. Feng, X.F. Feng, Y.W. Ding, X.Q. Liu, G.Y. Meng, Preparation of low-cost mullite ceramics from natural bauxite and industrial waste fly ash, J. Alloys Compd. 460 (2008) 599–606.
[22] Y.C. Dong, J.E. Zhou, B. Lin, Y.Q. Wang, S.L. Wang, L.F. Miao, Y. Lang, X.Q. Liu, G.Y. Meng, Reaction-sintered porous mineral-based mullite ceramic membrane supports made from recycled materials, J. Hazard. Mater. 172 (2009) 180–186.
[23] L. Montanaro, C. Perrot, C. Esnouf, G. Thollet, G. Fantozzi, A. Negro, Sintering of industrial mullites in the presence of magnesia as a sintering aid, J. Am. Ceram. Soc. 83 (2000) 189–196.
[24] D. Doni Jayaseelan, D. Amutha Rani, D. Benny Anburaj, T. Ohji, Pulse electric current sintering and microstructure of industrial mullite in the presence of sintering aids, Ceram. Int. 30 (2004) 539–543.
[25] Y.W. Kim, H.D. Kim, C.B. Park, Processing of microcellular mullite, J. Am. Ceram. Soc. 88 (2005) 3311–3315.
[26] M. Imose, A. Ohta, Y. Takano, M. Yoshinaka, K. Hirota, O. Yamaguchi, Low-temperature sintering of mullite/yttria-doped zirconia composites in the mullite-rich region, J. Am. Ceram. Soc. 81 (1998) 1050–1052.
[27] P. Sarin, W. Yoon, R.P. Haggerty, C. Chiritescu, N.C. Bhorkar, W.M. Kriven, Effect of transition-metal-ion doping on high temperature thermal expansion of 3:2 mullite—an in situ, high temperature, synchrotron diffraction study, J. Eur. Ceram. Soc. 28 (2008) 353–365.
[28] M. Caldwell, Role of titania in bauxite refractories, Brit. Ceram. Soc. Trans. 66 (1967) 107–119.
[29] X.C. Zhong, G.P. Li, Sintering characteristics of Chinese bauxites, Ceram. Int. 7 (1981) 65–68.
[30] H.S. Tripathi, G. Banerjee, Synthesis and mechanical properties of mullite from beach sandsillimanite: effect of TiO_2, J. Eur. Ceram. Soc. 18 (1998) 2081–2087.
[31] S.H. Hong, G.L. Messing, Mullite transformation kinetics in P_2O_5-, TiO_2-, and B_2O_3-doped aluminosilicate gels, J. Am. Ceram. Soc. 80 (1997) 1551–1559.
[32] E.R. Sola, F.J. Serrano, E. Delgado-Pinar, M.M. Reventĩos, A.I. Pardo, M.A. Kojdecki, J.M. Amigĩo, J. Alarcĩon, Solubility and microstructural development of TiO_2-containing $3Al_2O_3{\cdot}2SiO_2$ and $2Al_2O_3{\cdot}SiO_2$ mullites obtained from single-phase gels, J. Eur. Ceram. Soc. 27 (2007) 2647–2654.
[33] S.K. Sen, P.S. Aggarwal, Effect of TiO_2 and ZrO_2 on sintering of sillimanite, Ceram. Int. 20 (1994) 299–302.
[34] E. Jakobs, W.J. Koros, Ceramic membrane characterization via the bubble point technique, J. Membr. Sci. 124 (1997) 149–159.
[35] J.J.K. Mackenzie, R. Shuttleworth, A phenomenological theory of sintering, Proc. Phys. Soc. Lond. 62 (1949) 633–652.
[36] J.A. Pask, Importance of starting materials on reactions and phase equilibria in the Al_2O_3–SiO_2 system, J. Eur. Ceram. Soc. 16 (1996) 101–108.